Supporting Information

SI Materials and Methods

R_0 model extended mathematical framework

Equation 1 in the main text is a special case of the two hosts – two vectors R_0 derived in [1] and given below:

$$R_0 = \sqrt{\frac{1}{2}[(R_{11}+R_{22}) + \sqrt{(R_{11}+R_{22})^2 - 4(R_{11}R_{22}-R_{12}R_{21})}]}$$

where:

$$R_{11} = \left(\frac{b_1\beta_1 a_1^2}{\mu_1}\right)\left(\frac{\nu_1}{\nu_1+\mu_1}\right)\left(\frac{\phi_1^2 m_{A1}}{r_A+d_A} + \frac{(1-\phi_1)^2 m_{B1}}{r_B+d_B}\right)$$

$$R_{22} = \left(\frac{b_2\beta_2 a_2^2}{\mu_2}\right)\left(\frac{\nu_2}{\nu_2+\mu_2}\right)\left(\frac{\phi_2^2 m_{A2}}{r_A+d_A} + \frac{(1-\phi_2)^2 m_{B2}}{r_B+d_B}\right)$$

$$R_{12} = \left(\frac{b_2\beta_1 a_2 a_1}{\mu_2}\right)\left(\frac{\nu_2}{\nu_2+\mu_2}\right)\left(\frac{\phi_2\phi_1 m_{A1}}{r_A+d_A} + \frac{(1-\phi_2)(1-\phi_1) m_{B1}}{r_B+d_B}\right)$$

$$R_{21} = \left(\frac{b_1\beta_2 a_1 a_2}{\mu_1}\right)\left(\frac{\nu_1}{\nu_1+\mu_1}\right)\left(\frac{\phi_1\phi_2 m_{A2}}{r_A+d_A} + \frac{(1-\phi_1)(1-\phi_2) m_{B2}}{r_B+d_B}\right).$$

The subscripts 1 and 2 indicate vectors of type 1 and type 2, respectively. The subscripts *A* and *B* indicate hosts of type A and type B, respectively. The special case is obtained by taking the limit as r_B tends to infinity. This corresponds to preventing infection of the second host. As a result, the terms relating to the second host disappear and $R_{11}R_{22} - R_{12}R_{21}$ becomes zero. As the expression no longer involves two hosts, we can remove the subscript *A* and, as pathogen-induced mortality is zero for Zika, we can remove this parameter too.

Note that $\tilde{R}_{11}$ and $\tilde{R}_{22}$ in Equation 1 still contain ϕ_1 and ϕ_2, namely the proportion of vectors of type 1 and type 2, respectively, attracted to human hosts. Therefore, differences in feeding preferences between *A. aegypti* and *A. albopictus* can be taken into account. For completeness, we include below an explicit derivation, which need only include equations for the one true host.

Using the following equations based on [1], we can derive an expression for the R_0 of Zika. *X*, *Y* and *Z* represent the numbers of susceptible, infectious and recovered hosts. The total number of hosts is represented by *H*. S_i, L_i and I_i represent the numbers of susceptible, latent and infectious vectors of type *i*, where *i* can be either 1 (*A. aegypti*) or 2 (*A. albopictus*). The total numbers of vectors are represented by N_i. Note that for Zika there is only one main host capable of transmitting the infection and so only one set of host equations is given. In addition, there is no pathogen-induced mortality associated with Zika virus infection.

$$\frac{dX}{dt} = -\lambda_H X$$

$$\frac{dY}{dt} = \lambda_H X - rY$$
$$\frac{dZ}{dt} = rY$$

$$\frac{dS_i}{dt} = \rho_i N_i - \lambda_{Vi} S_i - \mu_i S_i$$
$$\frac{dL_i}{dt} = \lambda_{Vi} S_i - (\nu_i + \mu_i) L_i$$
$$\frac{dI_i}{dt} = \nu_i L_i - \mu_i I_i$$

where $\lambda_H = \sum_{i=\{1,2\}} b_i a_i \phi_i m_i I_i / N_i$ and $\lambda_{Vi} = \beta_i a_i \phi_i Y / H$.

Derivation of R_0

Let x be a vector containing the number of individuals in each compartment. Let $\Psi_p(x)$ be the rate at which new infections appear in compartment p and $\Phi_p(x)$ be the rate at which individuals leave compartment p (or, if the rate is negative, are added to compartment p by any other means).

$$\Psi = \begin{pmatrix} \lambda_H X \\ \lambda_{V1} S_1 \\ \lambda_{V2} S_2 \\ 0 \\ 0 \end{pmatrix} \qquad \Phi = \begin{pmatrix} rY \\ (\nu_1 + \mu_1) L_1 \\ (\nu_2 + \mu_2) L_2 \\ -\nu_1 L_1 + \mu_1 I_1 \\ -\nu_2 L_2 + \mu_2 I_2 \end{pmatrix}.$$

Note that there are five compartments: (1) infectious human hosts, Y; (2) latent vectors of type 1, L_1; (3) latent vectors of type 2, L_2; (4) infectious vectors of type 1, I_1, and (5) infectious vectors of type 2, I_2. R_0 is the dominant eigenvalue of the next-generation matrix K, which is given by $K = FV^{-1}$ where

$$F = \left[\frac{\partial \Psi_p}{\partial x_q}(x_0) \right], \qquad V = \left[\frac{\partial \Phi_p}{\partial x_q}(x_0) \right], \qquad 1 \le p, q \le 5.$$

The partial derivatives are evaluated at the disease-free equilibrium denoted by x_0. It follows that

$$K = \begin{pmatrix} 0 & k_{12} & k_{13} & k_{14} & k_{15} \\ k_{21} & 0 & 0 & 0 & 0 \\ k_{31} & 0 & 0 & 0 & 0 \\ 0 & 0 & 0 & 0 & 0 \\ 0 & 0 & 0 & 0 & 0 \end{pmatrix},$$

where k_{pq} is the number of new cases in compartment *p* produced by an infectious individual from compartment *q*. The elements of *K* are given in Table S2.

From $|K - \lambda I| = 0$, we find that R_0 is the largest solution of $\lambda^4 - \lambda^2(k_{21}k_{12} + k_{31}k_{13}) = 0$.

Hence $\lambda = \sqrt{k_{21}k_{12} + k_{31}k_{13}} = \sqrt{\frac{b_1\beta_1 a_1^2 \phi_1^2 \nu_1 m_1}{\mu_1(\nu_1 + \mu_1)r} + \frac{b_2\beta_2 a_2^2 \phi_2^2 \nu_2 m_2}{\mu_2(\nu_2 + \mu_2)r}}$.

This can be rewritten as

$$R_0 = \sqrt{\tilde{R}_{11} + \tilde{R}_{22}}$$

where

$$\tilde{R}_{11} = \left(\frac{b_1\beta_1 a_1^2}{\mu_1}\right)\left(\frac{\nu_1}{\nu_1 + \mu_1}\right)\left(\frac{\phi_1^2 m_1}{r}\right)$$
$$\tilde{R}_{22} = \left(\frac{b_2\beta_2 a_2^2}{\mu_2}\right)\left(\frac{\nu_2}{\nu_2 + \mu_2}\right)\left(\frac{\phi_2^2 m_2}{r}\right).$$

SI Tables

Table S1. Number of reported dengue occurrence points inside and outside the environmental envelope of ZIKV transmission (see Fig S1). The model environmental envelope is defined for mean annual R_0 values (for the period 1980-2015) exceeding the 1 threshold.

	Number of points inside (n, %)	Number of points outside (n, %)	Total number of points
All spatial points	6446 (77.5)	1869 (22.5)	8306
Points excluding Tropical islands (which are not included in the model due to the coarse spatial resolution of the climate data e.g. 0.5° x 0.5° degrees).	6437 (95.9)	278 (4.1)	6715

Table S2. Elements of next generation matrix K

Elements for vector species 1	**Formula**	**Elements for vector species 2**	**Formula**
k_{12}	$\frac{b_1 a_1 \phi_1 \nu_1}{\mu_1(\nu_1+\mu_1)}$	k_{13}	$\frac{b_2 a_2 \phi_2 \nu_2}{\mu_2(\nu_2+\mu_2)}$
k_{14}	$\frac{b_1 a_1 \phi_1}{\mu_1}$	k_{15}	$\frac{b_2 a_2 \phi_2}{\mu_2}$
k_{21}	$\frac{\beta_1 a_1 \phi_1 m_1}{r}$	k_{31}	$\frac{\beta_2 a_2 \phi_2 m_2}{r}$

SI figures

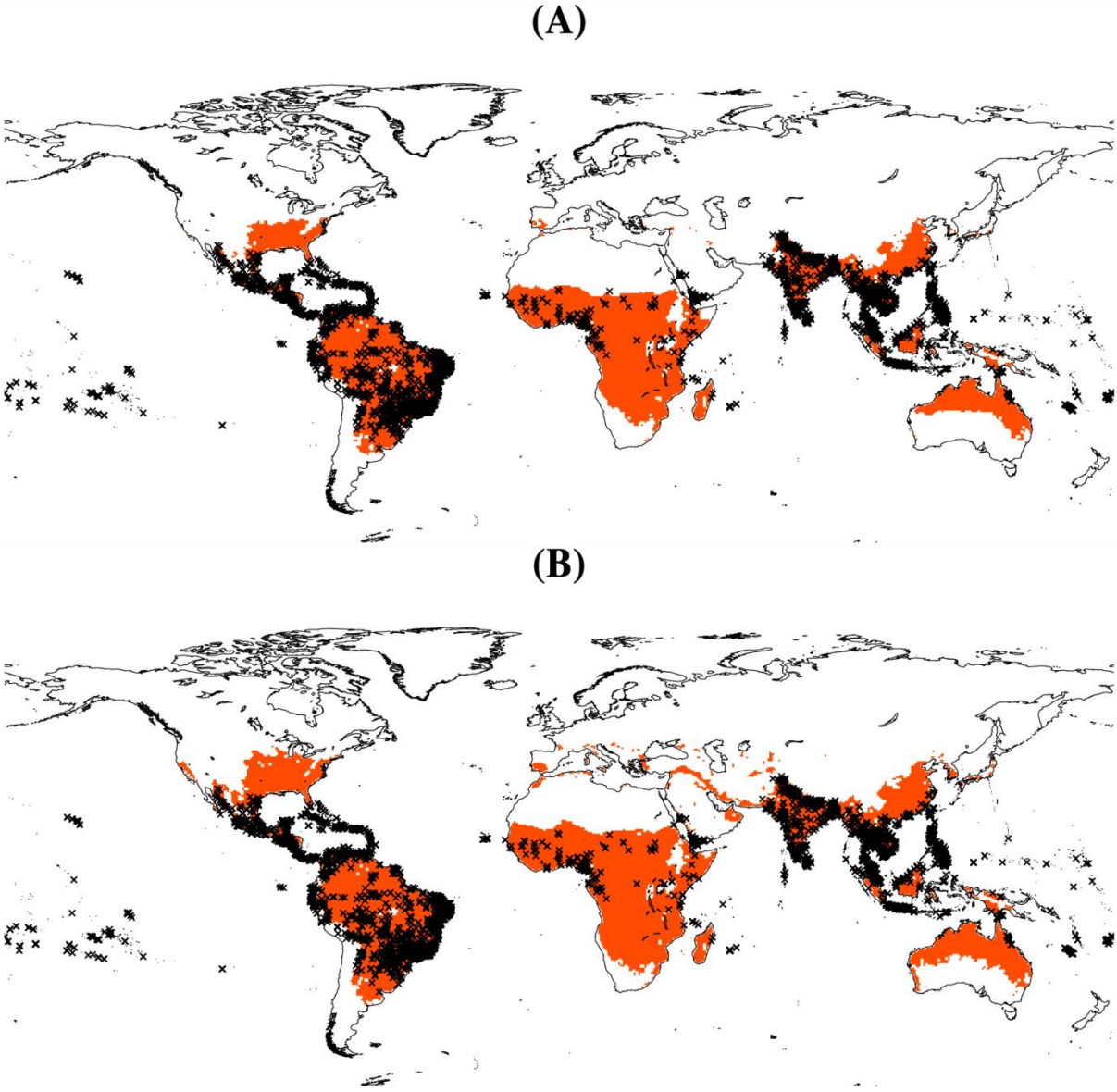

Fig. S1. Regions where R_0 >1 (orange shading). This is carried out for the (A) annual mean (1980-2015) and for (B) the R_0 peak (monthly maximum over the 1980-2015 period). The black crosses depict occurrence of dengue virus based on [2].

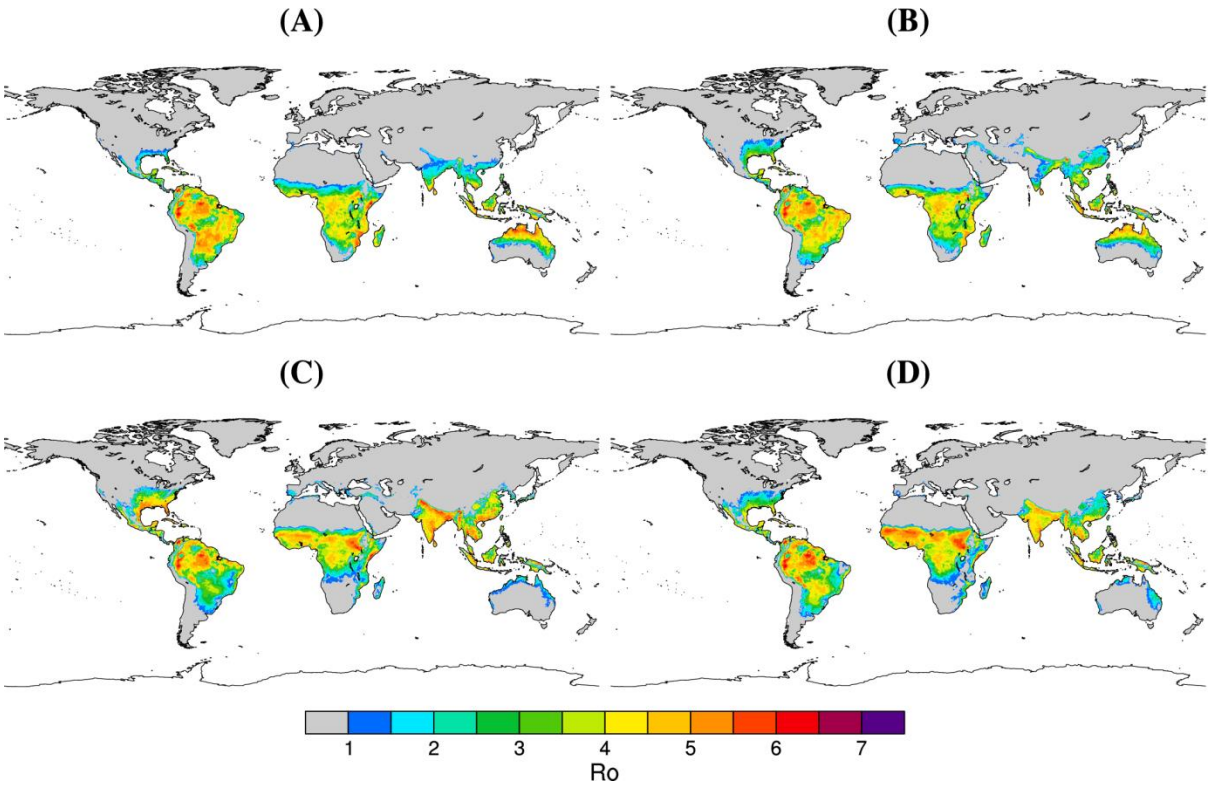

Fig. S2. R_0 seasonal changes for (A) boreal winter (Dec-Jan-Feb), (B) spring (Mar-Apr-May), (C) summer (Jun-Jul-Aug) and (D) autumn (Sep-Oct-Nov) at **global** scale. The seasonal mean is calculated for the period 1980-2015.

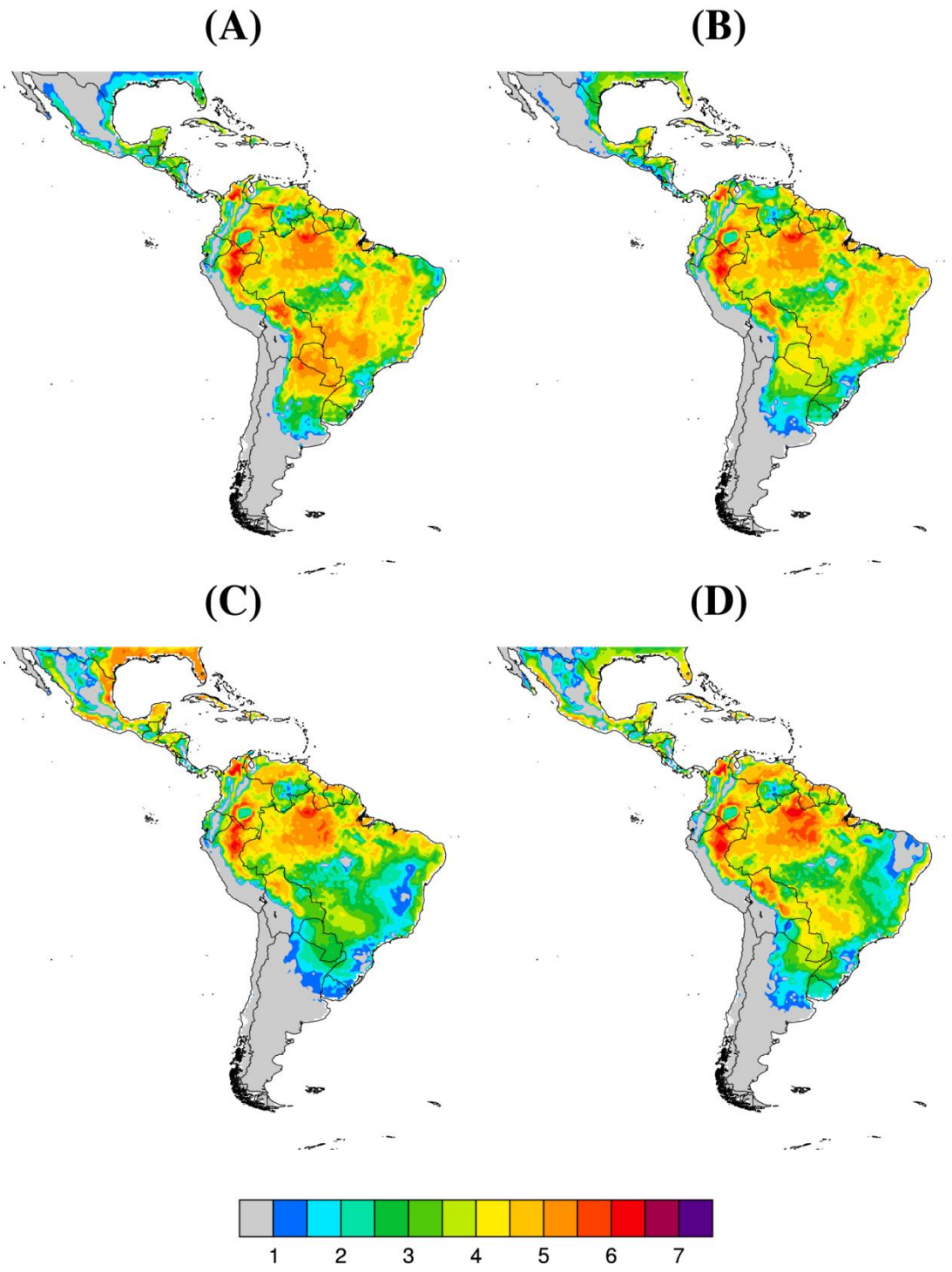

Fig. S3. R_0 seasonal changes for (A) boreal winter (Dec-Jan-Feb), (B) spring (Mar-Apr-May), (C) summer (Jun-Jul-Aug) and (D) autumn (Sep-Oct-Nov) for **Latin America**. The seasonal mean is calculated for the period 1980-2015.

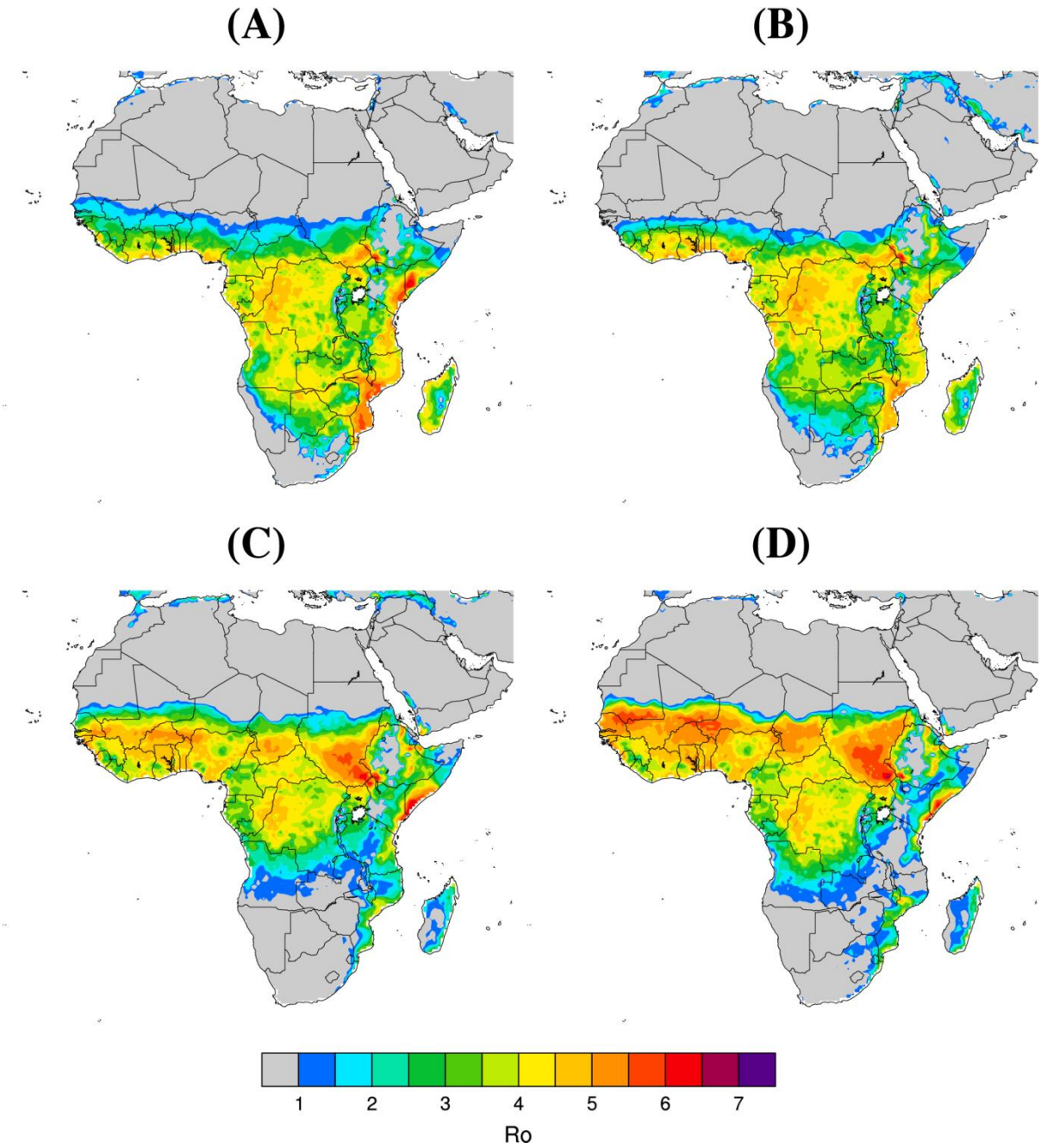

Fig. S4. R_0 seasonal changes for (A) boreal winter (Dec-Jan-Feb), (B) spring (Mar-Apr-May), (C) summer (Jun-Jul-Aug) and (D) autumn (Sep-Oct-Nov) for **Africa**. The seasonal mean is calculated for the period 1980-2015.

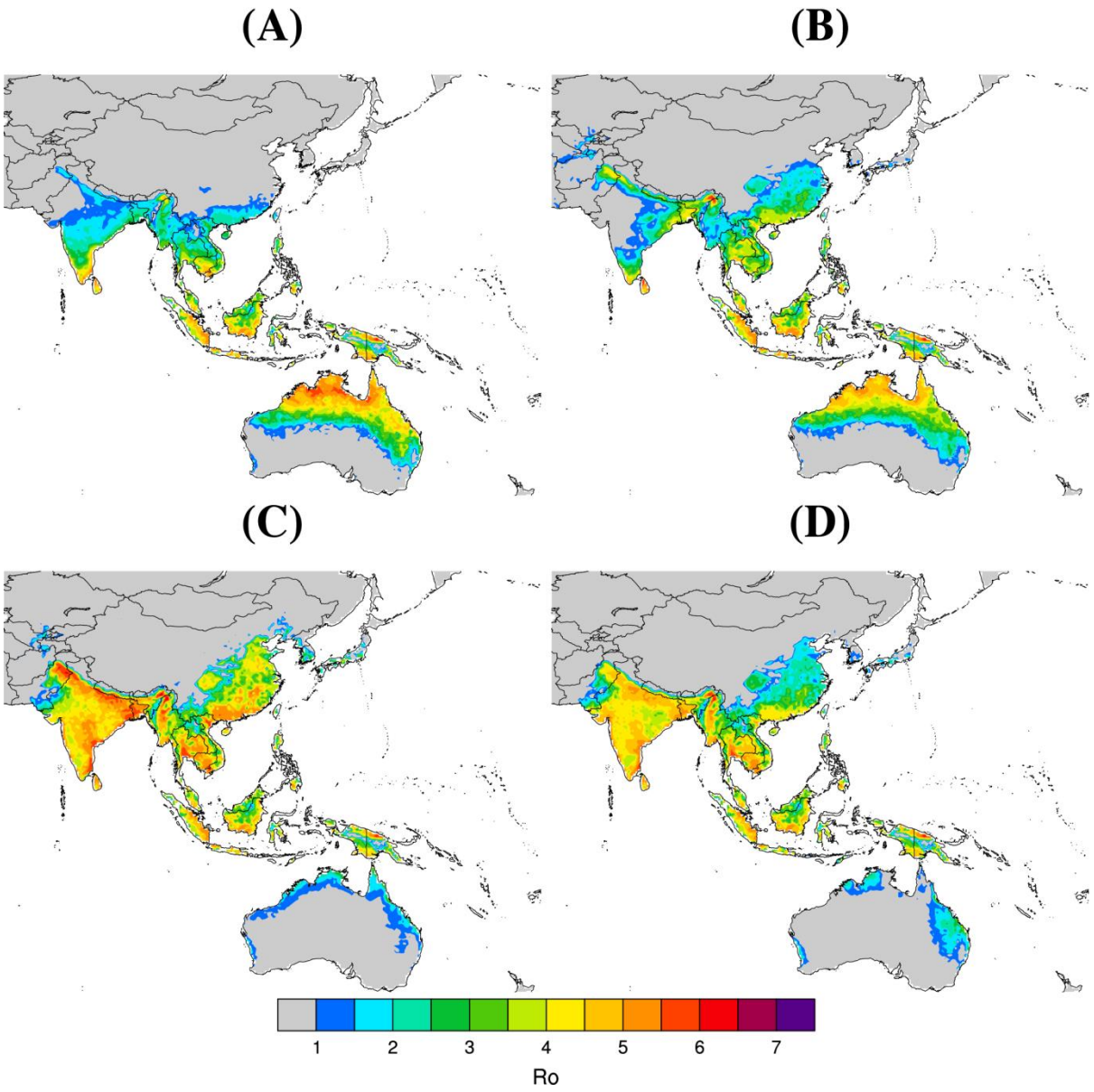

Fig. S5. R_0 seasonal changes for (A) boreal winter (Dec-Jan-Feb), (B) spring (Mar-Apr-May), (C) summer (Jun-Jul-Aug) and (D) autumn (Sep-Oct-Nov) for **Asia and Oceania**. The seasonal mean is calculated for the period 1980-2015.

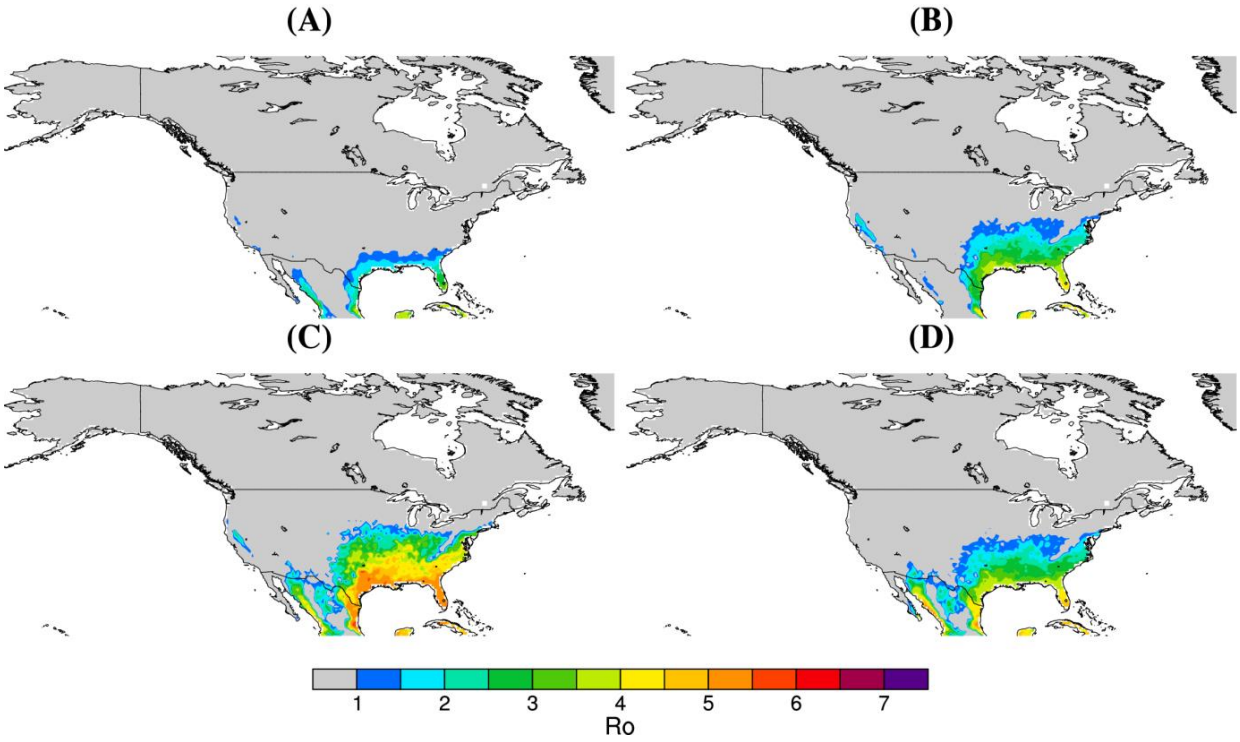

Fig. S6. R_0 seasonal changes for (A) boreal winter (Dec-Jan-Feb), (B) spring (Mar-Apr-May), (C) summer (Jun-Jul-Aug) and (D) autumn (Sep-Oct-Nov) for **North America**. The seasonal mean is calculated for the period 1980-2015.

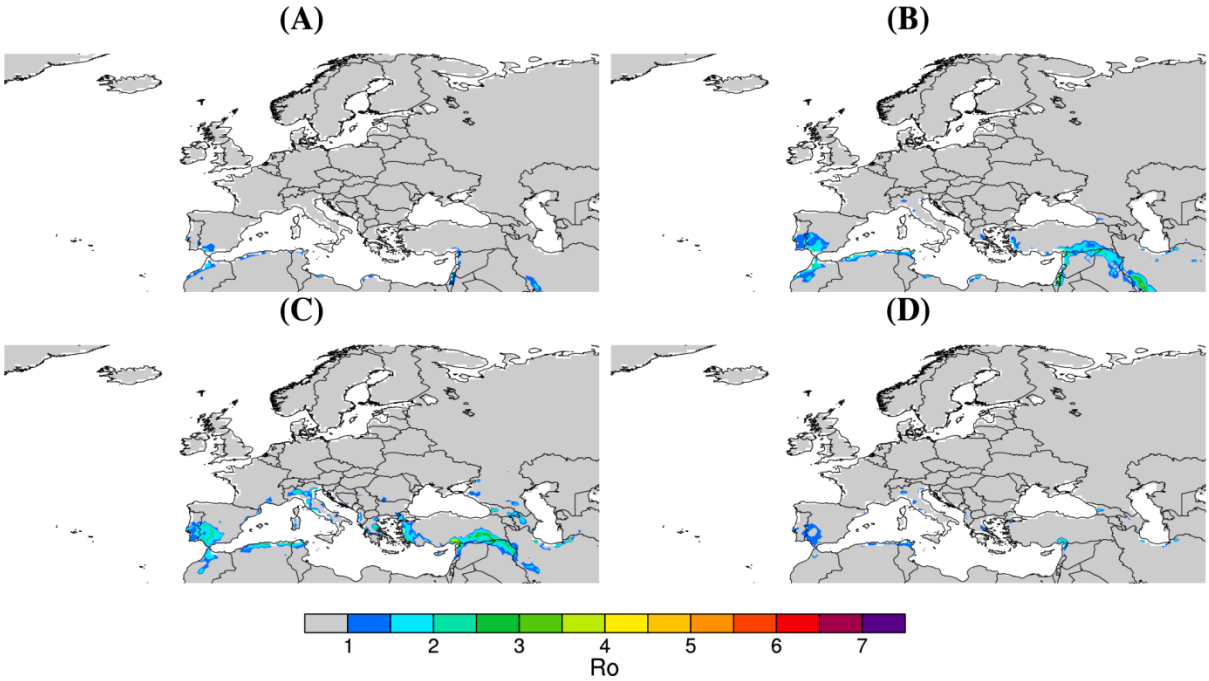

Fig. S7. R_0 seasonal changes for (A) boreal winter (Dec-Jan-Feb), (B) spring (Mar-Apr-May), (C) summer (Jun-Jul-Aug) and (D) autumn (Sep-Oct-Nov) for **Europe**. The seasonal mean is calculated for the period 1980-2015.

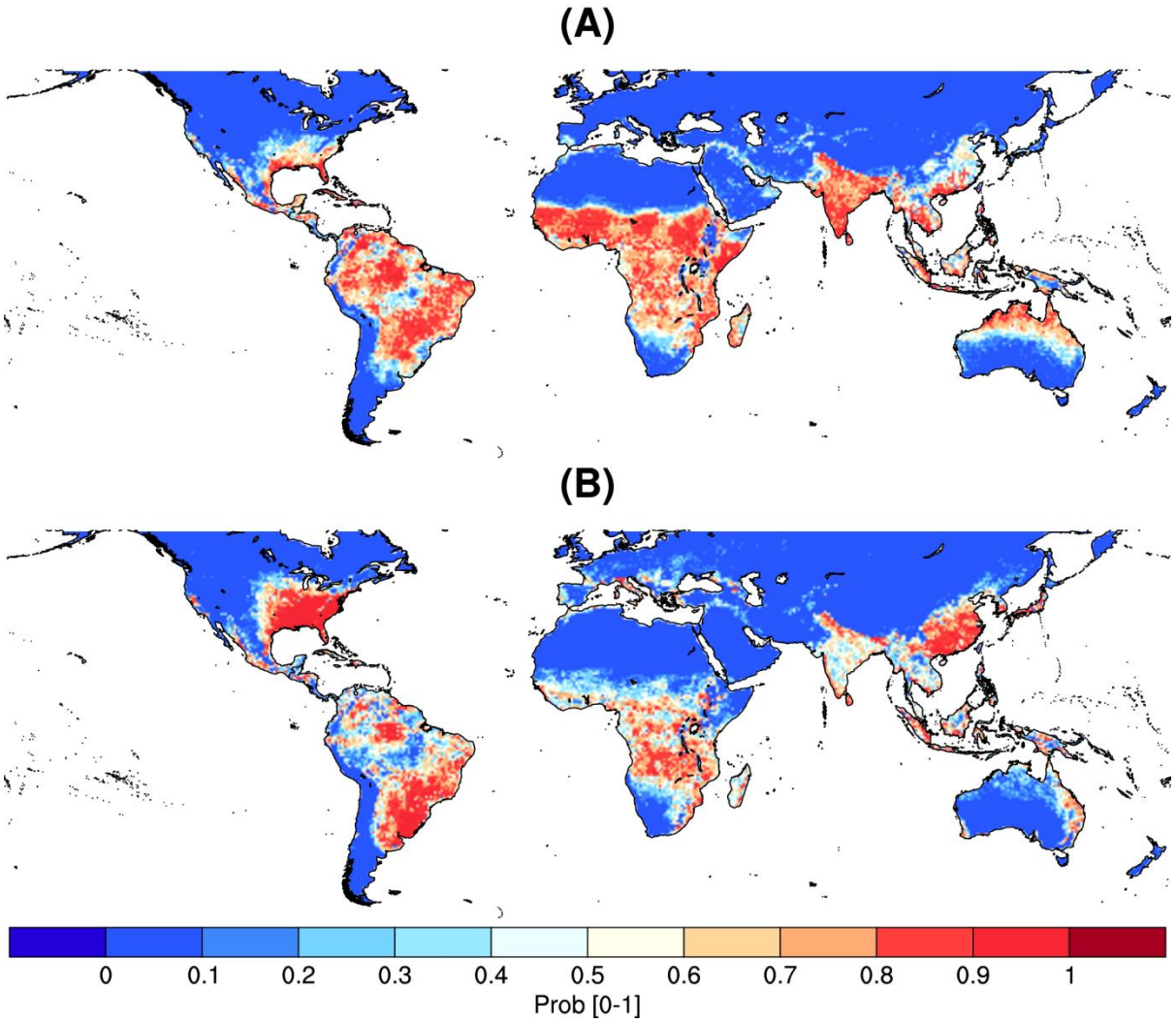

Fig. S8. Global probability of occurrence for (A) *Ae. aegypti* and (B) *Ae. albopictus* – based on the modelling work by [3].

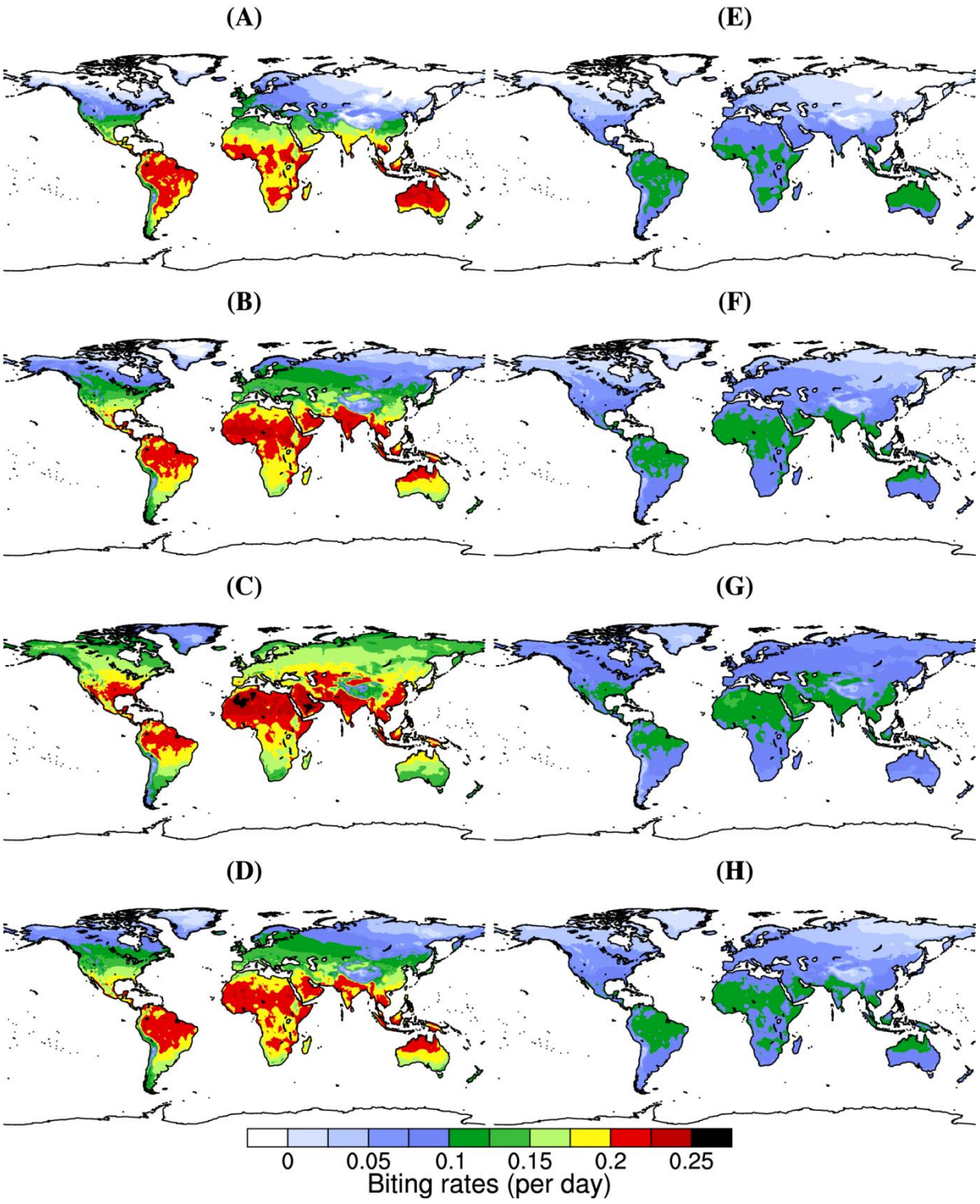

Fig. S9. Biting rate seasonal changes for boreal winter (A for *Ae.aegypti* and E for *Ae. albopictus*), spring (B for *Ae.aegypti* - F for *Ae. albopictus*), summer (C for *Ae.aegypti* - G for *Ae. albopictus*) and autumn (D for *Ae.aegypti* - H for *Ae. albopictus*). The average is calculated for the period 1980-2015.

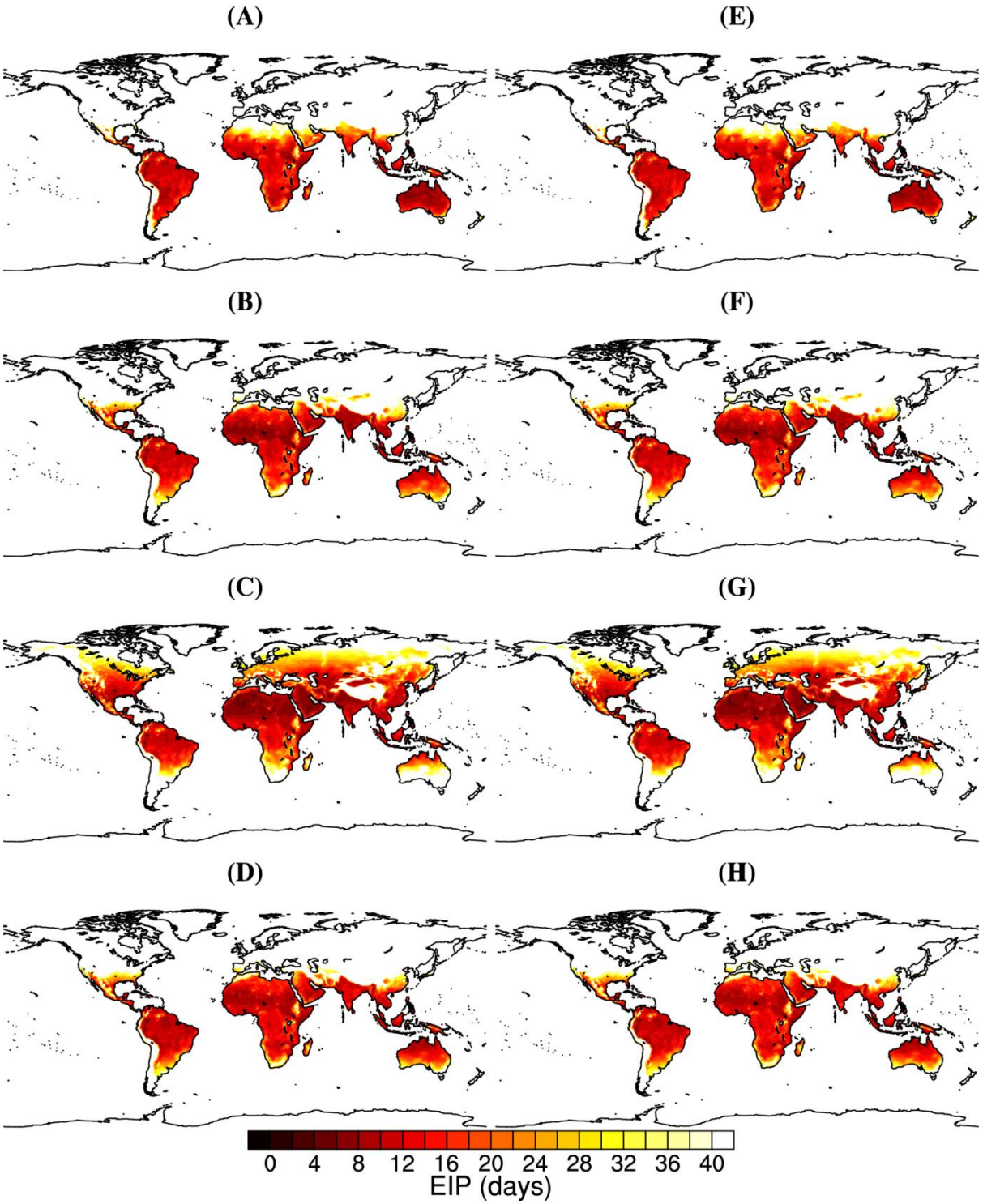

Fig. S10. Extrinsic Incubation Period (EIP) seasonal changes for boreal winter (A for *Ae.aegypti* - E for *Ae. albopictus*), spring (B for *Ae.aegypti* - F for *Ae. albopictus*), summer (C for *Ae.aegypti* - G for *Ae. albopictus*) and autumn (D for *Ae.aegypti* - H for *Ae. albopictus*). The average is calculated for the period 1980-2015.

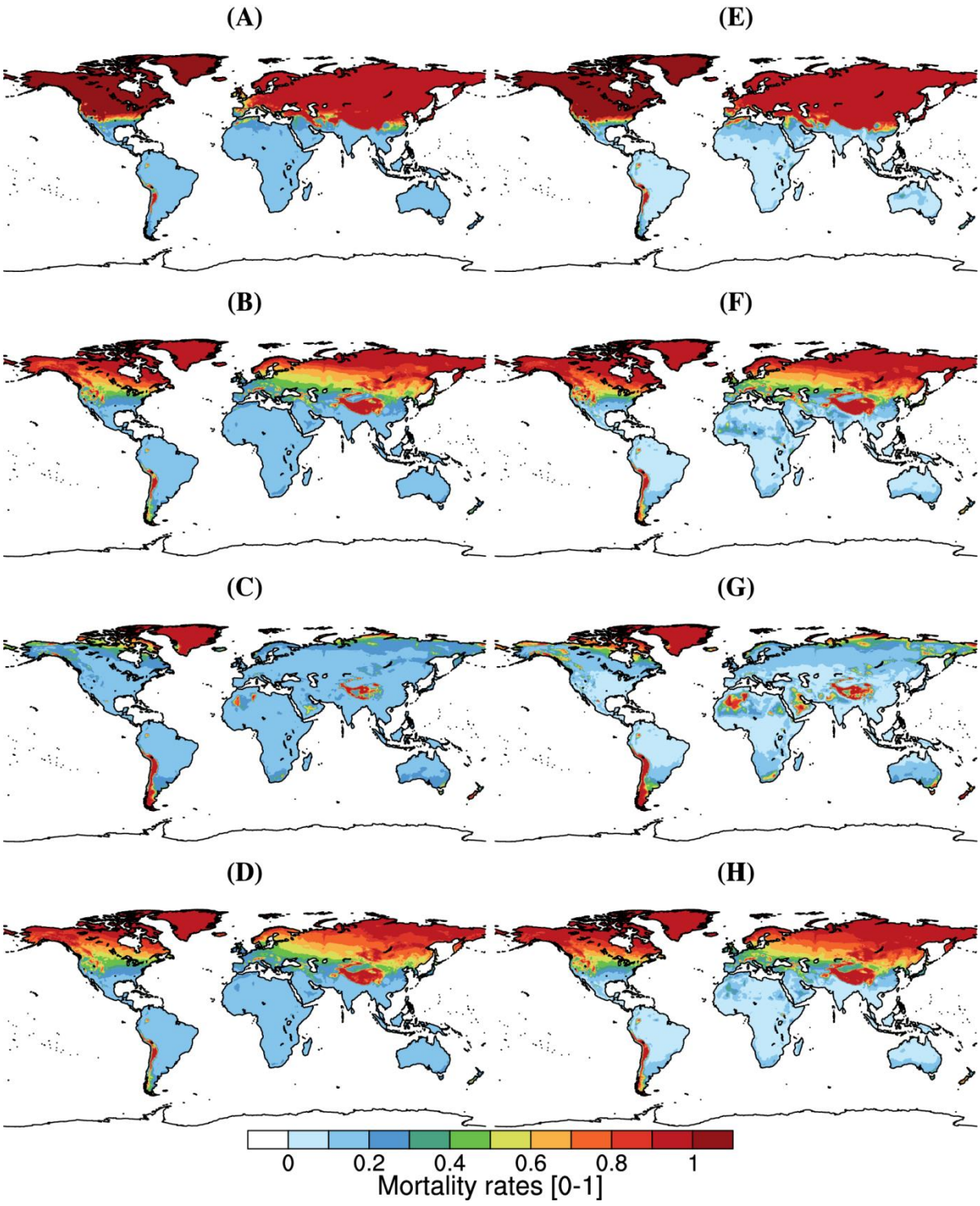

Fig. S11. Mortality rates seasonal changes for boreal winter (A for *Ae.aegypti* - E for *Ae. albopictus*), spring (B for *Ae.aegypti* - F for *Ae. albopictus*), summer (C for *Ae.aegypti* - G for *Ae. albopictus*) and autumn (D for *Ae.aegypti* - H for *Ae. albopictus*). The average is calculated for the period 1980-2015.

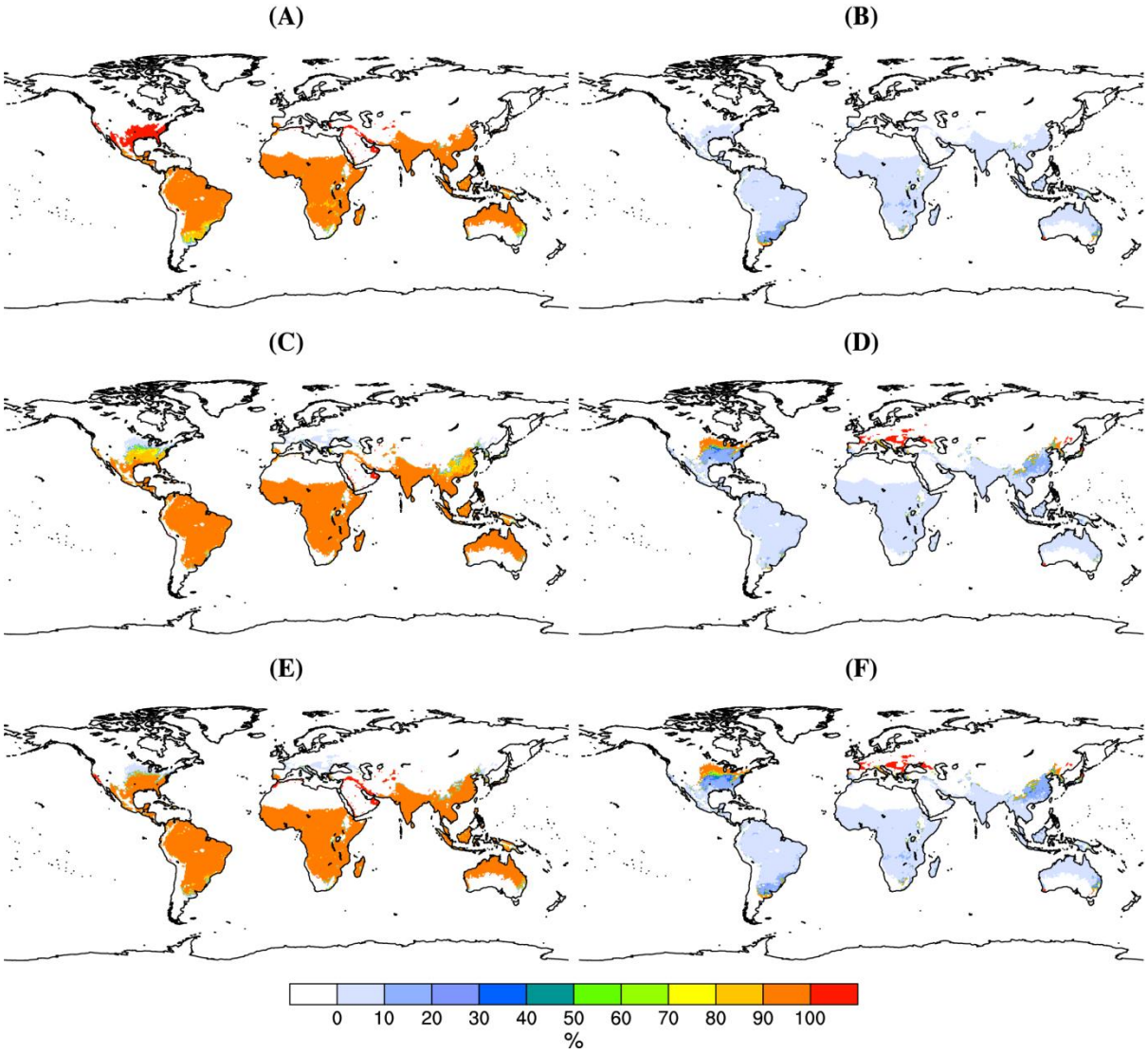

Fig S12. Relative contribution of R_{11} (*Ae. Aegypti*, left column) and R_{22} (*Ae. Albopictus*, right column) to R_0 (%). These are carried out for boreal winter (A & B), boreal summer (C & D) and for the annual mean (E & F) for the period1980-2015.

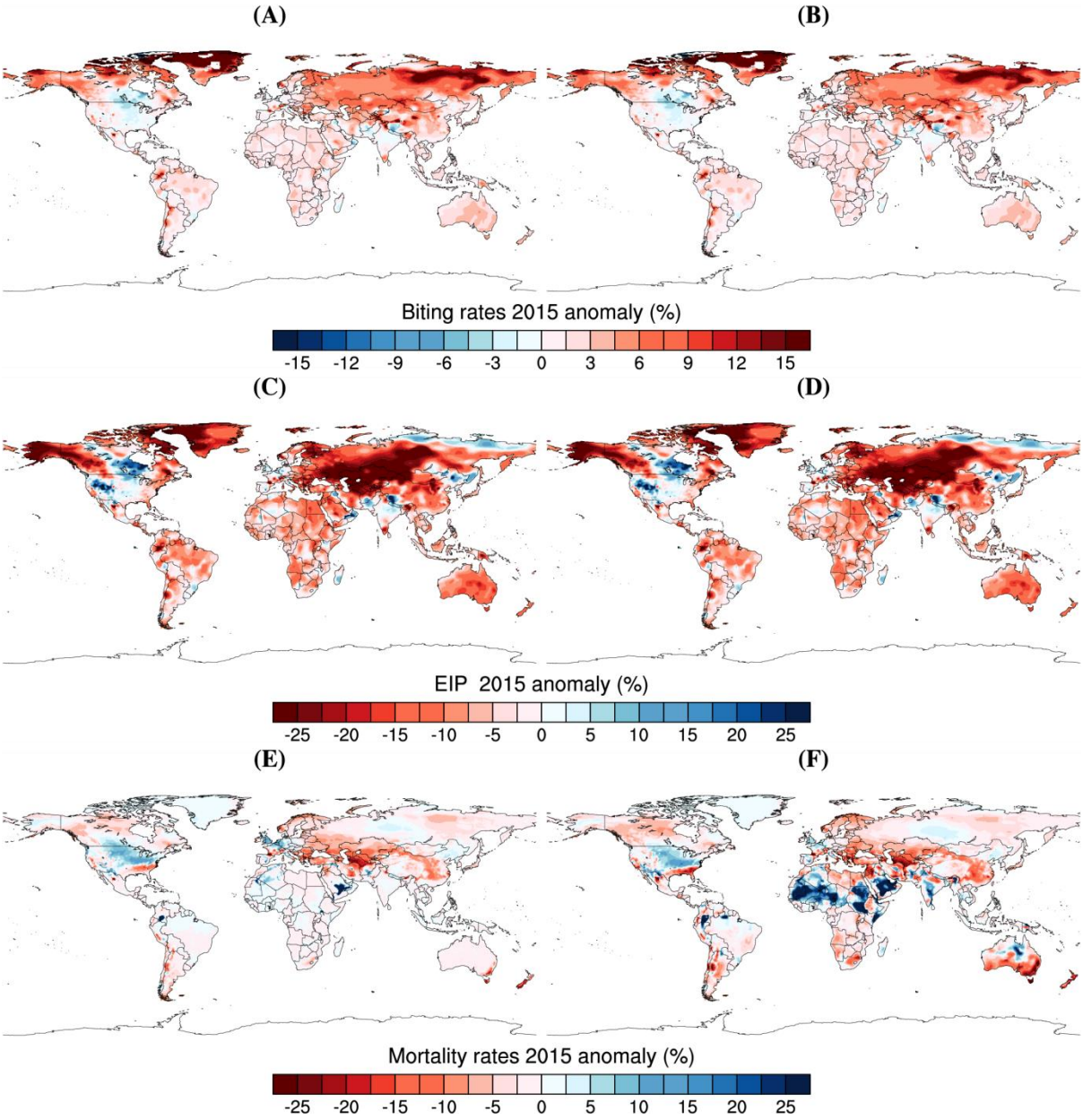

Fig S13. Biting rates (A for *Ae. aegypti* – B for *Ae. albopictus*), EIP (C for *Ae. aegypti* – D for *Ae. albopictus*) and Mortality rates (E for *Ae. aegypti* – F for *Ae. albopictus*) anomalies for 2015 (%). The reference climatology to calculate the anomaly is 1950-2015.

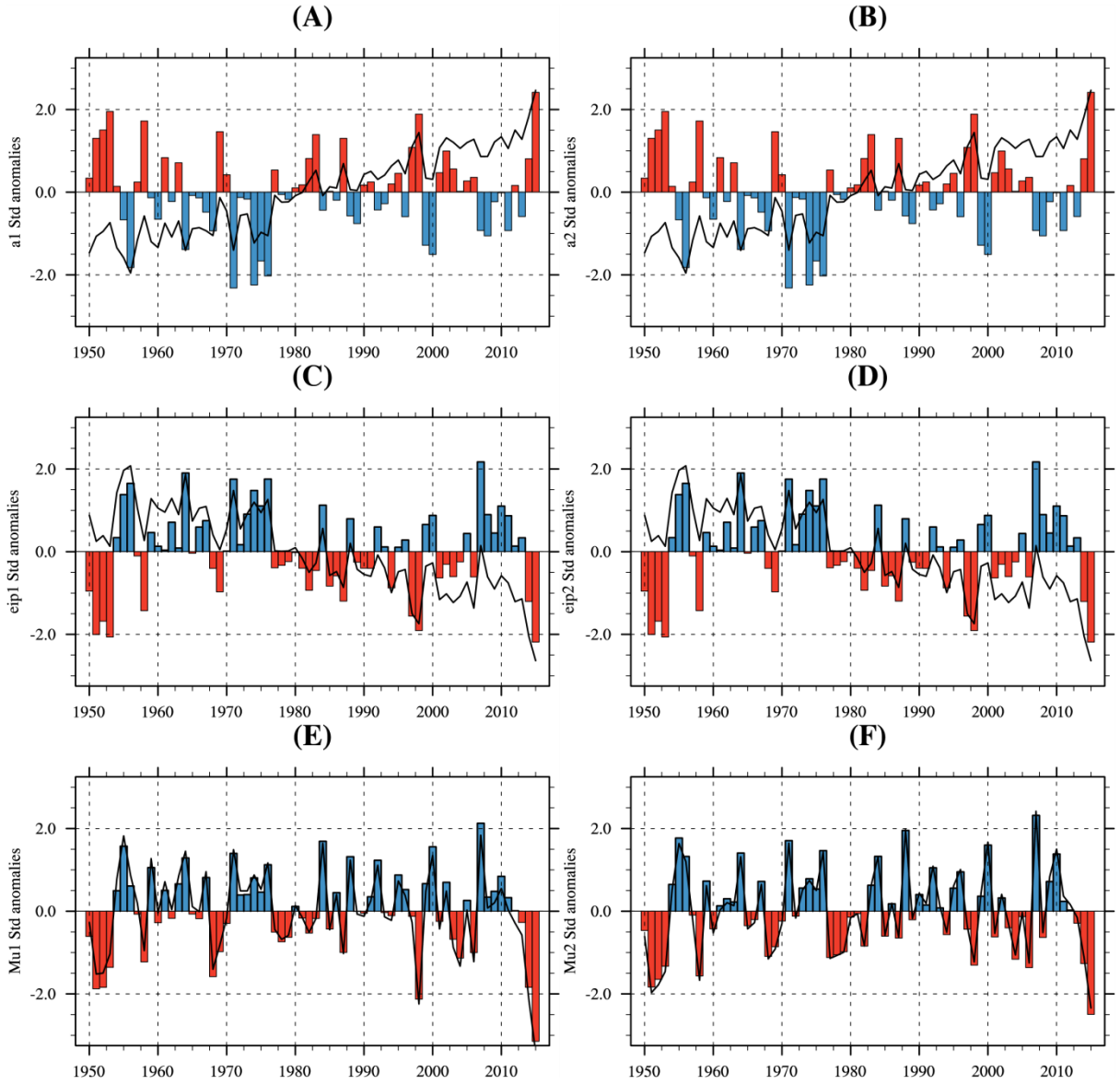

Fig S14. Biting rates (A & B), EIP (C & D) and Mortality rates (E & F) standardized anomalies for *Ae. aegypti* (left) and *Ae. albopictus* (right). The indices have been calculated for the South American continent, see Fig 1A) for the spatial domain definition. The solid line and the coloured bars respectively depict raw and linearly de-trended anomalies.

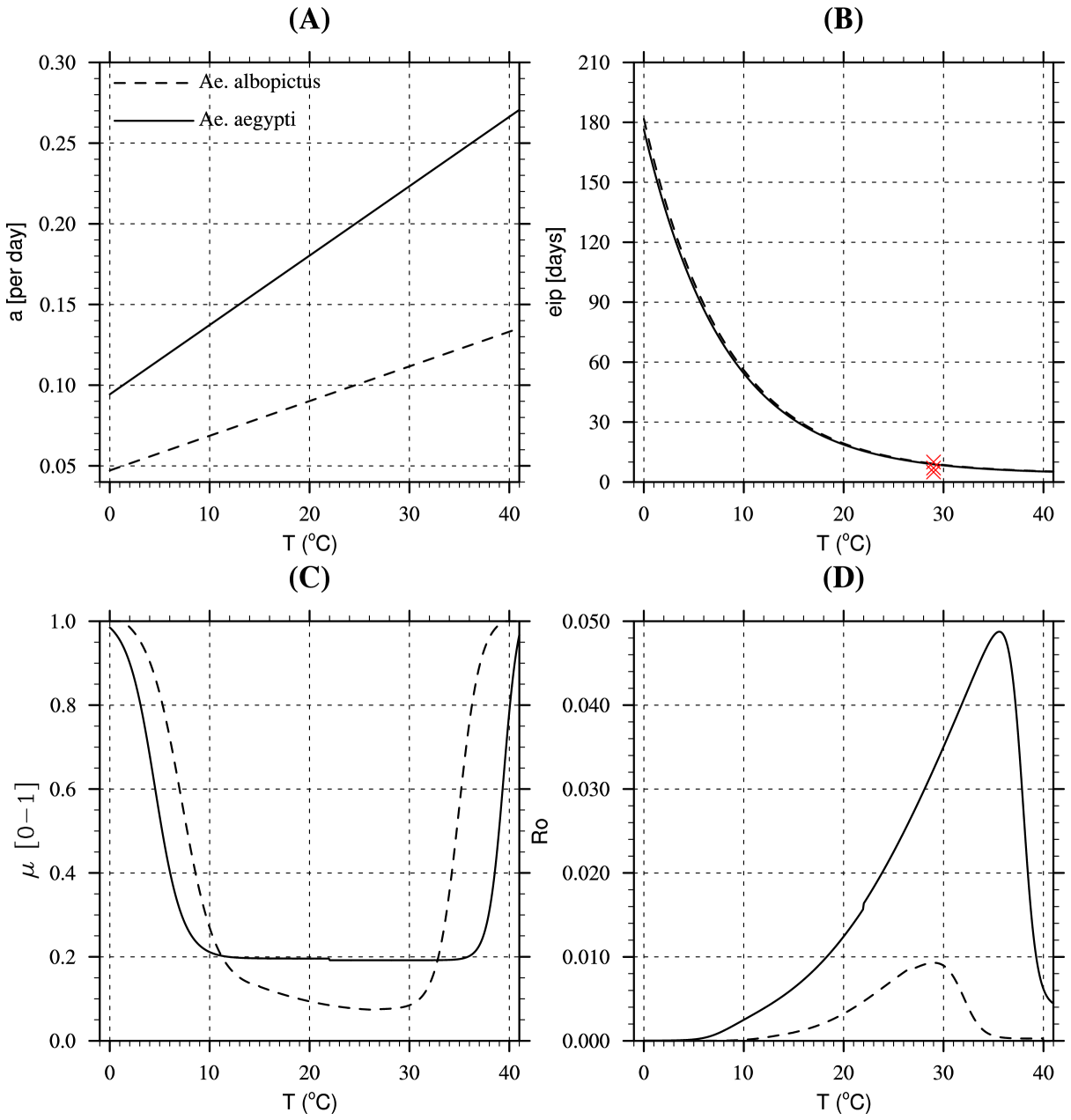

Fig. S15. Dependency of (A) biting rates, (B) extrinsic incubation periods, (C) mortality rates to temperature for *Ae. aegypti* and *Ae. albopictus*. The red crosses depict laboratory values for the EIP of ZIKV at 29°C following [4] and [5]. (D) R_0 model dependence to temperature which combines the three former parameters.

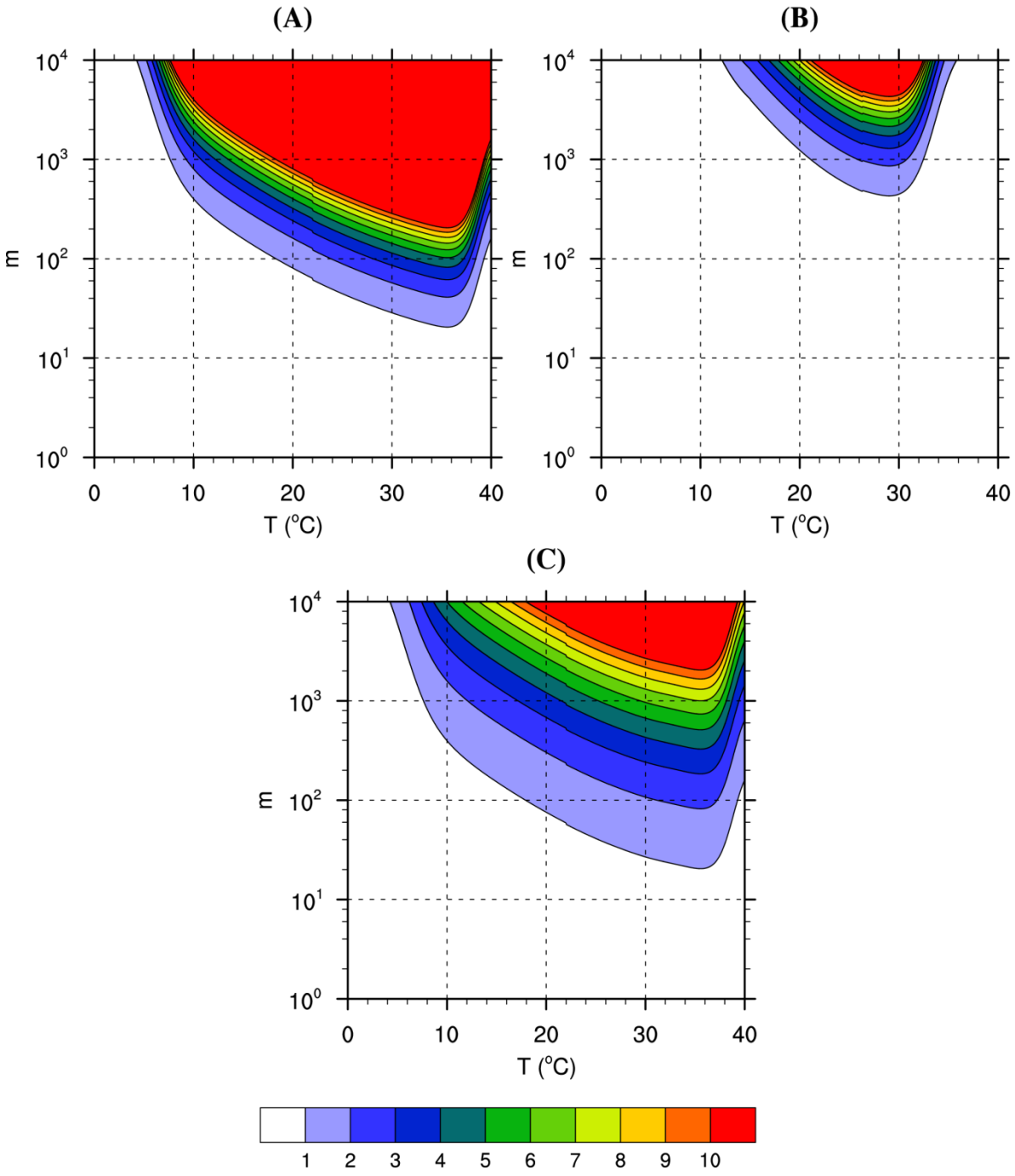

Fig. S16. (A) R_{11}, (B) R_{22} and (C) R_0 dependence to m and temperature.

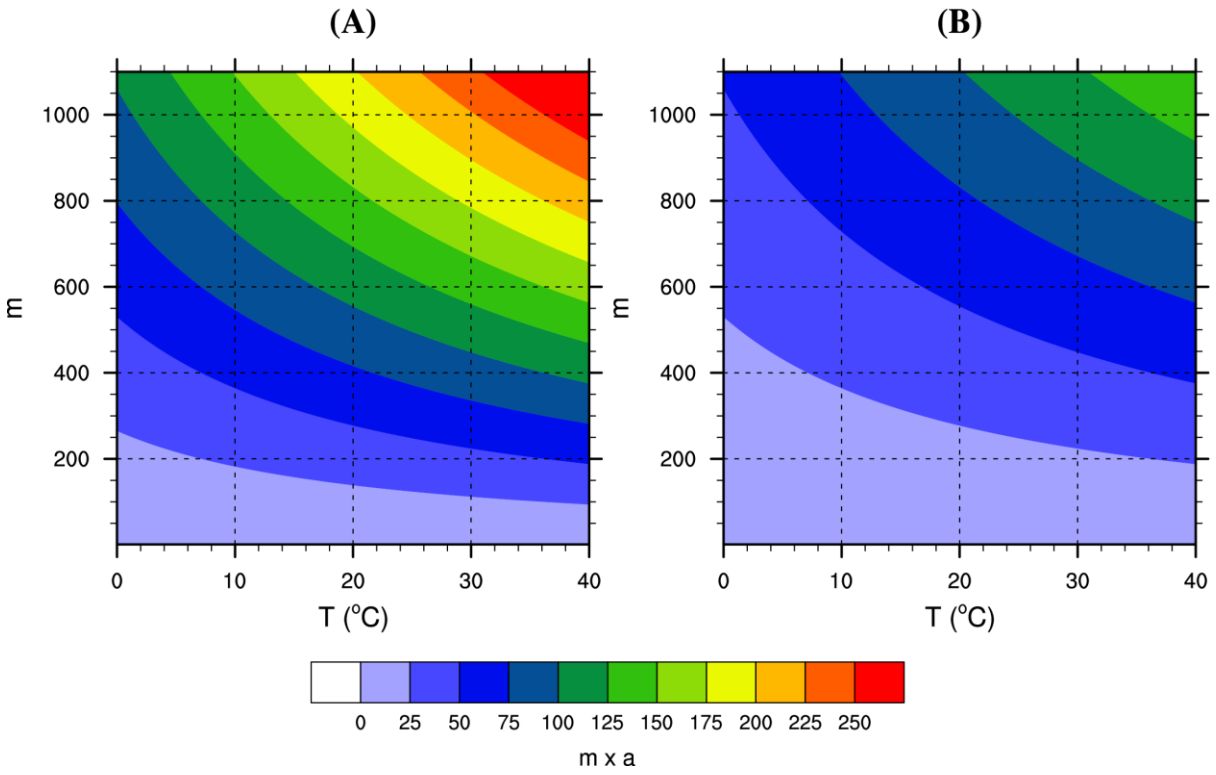

Fig. S17. m x a (number of mosquito bites per person per day) dependence to m and temperature for (A) *Ae. aegypti* and (B) *Ae. albopictus*.

References

1. Turner, J., R.G. Bowers, and M. Baylis, *Two-host, two-vector basic reproduction ratio (R(0)) for bluetongue.* PLoS One, 2013. **8**(1): p. e53128.
2. Bhatt, S., et al., *The global distribution and burden of dengue.* Nature, 2013. **496**.
3. Kraemer, M.U.G., et al., *The global distribution of the arbovirus vectors Aedes aegypti and Ae. albopictus.* eLife, 2015. **4**: p. e08347.
4. Li, M.I., et al., *Oral Susceptibility of Singapore Aedes (Stegomyia) aegypti (Linnaeus) to Zika Virus.* PLoS Neglected Tropical Diseases, 2012. **6**(8): p. e1792.
5. Chouin-Carneiro, T., et al., *Differential Susceptibilities of <italic>Aedes aegypti</italic> and <italic>Aedes albopictus</italic> from the Americas to Zika Virus.* PLoS Negl Trop Dis, 2016. **10**(3): p. e0004543.